Single Mol. **2** (2001) 2, 75-78

Molecular Recognition and Adhesion of Individual DNA Strands Studied by Dynamic Force Microscopy

Wilfried Grange, Torsten Strunz, Irina Schumakovitch, Hans-Joachim Güntherodt and Martin Hegner.

Department of Physics and Astronomy
National Center of Competence in Research (NCCR) on Nanoscale Science,
Klingelbergstr. 82,
University of Basel, CH-4056 Basel, Switzerland

Correspondence to
Martin Hegner
Department of Physics and Astronomy
University of Basel, CH-4056 Basel, Switzerland
phone: ++41-61-267 37 61
fax: ++41-61-267 37 84
e-mail: Martin.Hegner@unibas.ch

submitted 14 May 2001
accepted 26 June 2001
published 30 June 2001

Abstract

The development of versatile scanning probe methods such as atomic force microscopy (AFM) makes it today possible to study bio-adhesion on a single molecule level. In this paper, we present AFM-force-spectroscopy experiments on complementary DNA strands. From such experiments, intrinsic thermodynamical properties (energy landscape) of these weak non covalent bonds can be determined.

Introduction

It has long been known that only molecules with an excess of energy over the average energy of the population can participate in chemical reactions. Accordingly, reactions between ligands and receptors follow pathways (in a virtual energy landscape) that involve the formation of some type of high-energy transition states whose accessibility along a reaction coordinate ultimately controls the rate of the reaction. Until recently, chemists and biologists could only act on molecules if these were present in large quantities. Consequently, scientists could only access macroscopic thermodynamical quantities, e.g. the free energy of complex formation and/or dissociation.

Today, instruments offering a high spatial resolution and a sensitivity down to the pico- or femto-Newton range allow one to study the adhesion of molecular bonds [1-13]. In particular, a novel type of force spectroscopy, dynamic force microscopy (DFS), has been developed. In a DFS experiment, the dependence of the rupture force on the loading rate is investigated using an atomic force microscope (AFM), a bio-membrane force probe (BFP), or eventually an optical tweezers setup. For a typical DFS experiment using an AFM, a ligand is immobilized on a sharp tip attached to a micro-fabricated cantilever and the receptor is immobilized on a surface. When approaching the surface of the tip a bond may form between ligand and receptor. The bond is then loaded with an increasing force when retracting the surface from the tip. From these measurements, the energy landscape of a single bond can be mapped.

This paper is organized as follows: Part one introduces theoretical models that describe a chemical reaction when an external force is used to rupture a complex. Then, DFS experiments on complementary DNA strands are presented and illustrate the main ideas developed in part one.

Theoretical Background

In this section, some thermodynamical models describing the rupture of a single bond will be briefly presented. More details can be found elsewhere [15-18].

Bell first stated that the bond lifetime τ of an energy barrier reads:

$$\tau(F) = \tau_0 \exp\left[\left(E_0 - \Delta x F \right) / k_B T \right] \quad (1),$$

where T is the temperature, E_0 represents the bond energy (the height of the barrier), F is the external applied force per bond, k_B is the Boltzmann constant, Δx is the distance (projected along the direction of the applied force) between the ground state and the energy barrier (with energy E_0), and τ_0 is a pre-factor. Eq. (1) states that (i) a bond will rupture after a certain amount of time thanks to thermal fluctuations (ii) application of an external force dramatically changes the time it takes to overcome the energy barrier. Note finally that (1) can be re-written as:

$$k_{off}(F) = k_{off} \exp\left(F / F^0 \right) \quad (2),$$

where k_{off} is the thermal off-rate of the barrier, and F^0 is a force-scale factor ($F^0 = k_B T / \Delta x$).

An important point is that the most probable force F^* needed to overcome an energy barrier should *a priori* depend on the loading rate, *i.e.* the velocity in a typical DFS experiment (typical values for velocities are in the range between 10 nm/s and 5000 nm/s). Indeed, when the loading rate decreases, F^* should decreases because of thermal fluctuations. In fact, a simple relation holds between F^* and the loading rate r ($r = kv$, where k is the stiffness of the DFS force sensor and v is the retraction speed):

$$F^* = F^0 \ln\left(r \,/\, F^0 \; k_{off} \right) \quad (3),$$

By plotting F^* as a function of ln(r), one should therefore find different linear regimes, each of them corresponding to a specific region (a specific energy barrier) of the energy landscape. According to Evans [17], the kinetics runs as follows: application of an external force (i) selects a specific path (a reaction coordinate) in the energy landscape (ii) suppresses outer barriers (Eq. 1) and reveal inner barriers which start to govern the process. For instance, recent BFP and AFM experiments have revealed an intermediate state for the streptavidin (or avidin)-biotin complex [10, 13]. However, since each energy barrier defines a time-scale (a range of loading rate that has to be compatible with the time-scale of the experiment) only a specific part of the energy landscape can be mapped in a typical DFS experiment [18 - 19].

Experimental

DFS measurements were performed using a commercial AFM instrument (Nanoscope III, Digital Instruments, Santa Barbara). The spring constants of all cantilevers (ranging from 12 to 17 pN/nm) were calibrated by the thermal fluctuation method [20] with an absolute uncertainty of 20 %. For the temperature measurements presented below, the temperature was controlled using a home built cell where the buffer solution that immersed both the probe surface and the AFM cantilever was in contact with a Peltier element (Melcor, Trenton, NJ), driven with a constant current source. Measurements at different points of the cell showed deviations of less than 2 °C.

All chemicals were purchased from Fluka unless noted elsewhere. The preparation and immobilization of all oligonucleotides follow the protocol described in ref. 11.

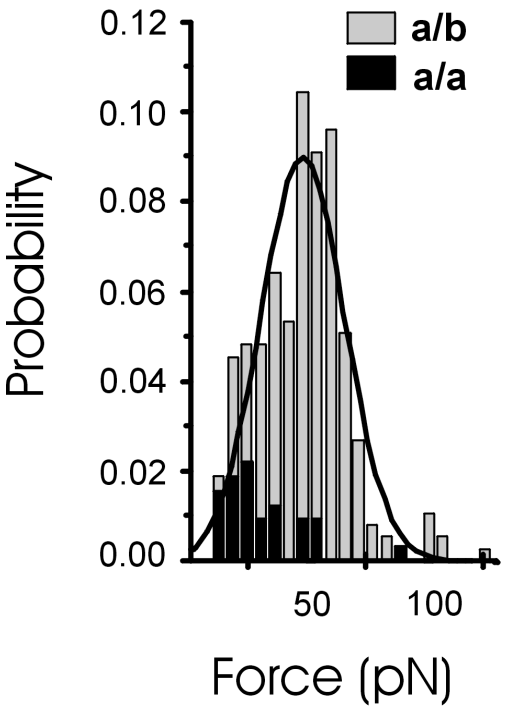

Fig. 1. *A typical probability distribution for the rupture force (about 500 approach/retract cycles, retract velocity 100 nm/s) [11]. For this experiment, an oligomer a (see text) was attached to the tip of the AFM-cantilever and its complement b was immobilized on the surface (complements were pulling apart at their opposite 5'-ends). Gray rectangles (***a** *against* **b**), *black rectangles (***a** *against* **a**). *To minimize unspecific interactions and multiple unbinding events, 30-nm-long PEG linkers were attached to the 5'-ends. Note that the scale-force F^0 can be in principle determined from the width of the distribution.*

Results and Discussion

Probability Distribution and Specificity of Rupture Forces

Unbinding events are caused by thermal fluctuations rather than by mechanical instability. Therefore unbinding forces show a distribution whose width σ is mainly determined by the force scale F^0, *i.e.* $\sigma=F^0(\Delta x)$.

When approaching the tip to the surface, many non-specific attachments may occur, even in the presence of treated surfaces or pure polymer samples. Therefore, it is imperative to test the specificity of the interaction (Fig. 1.). Unspecific interactions can be minimized using linkers (e.g. poly(ethylene)glycol (PEG) linkers) that shift the region where unbinding takes place away from the surface.

Finally, to quantify the most probable value for the unbinding force of a single complex, one has to work under conditions in which the probability that two or more duplexes are attached to the tip is low. These conditions are fulfilled for a low concentration and when the linkers have a length that is comparable to the diameter of the AFM-tip (about 50 nm). In this case, it is very unlikely that two or more linkers are extended to the same length when stretched. However, subsequent rupture events may be found. But still, the last rupture event will occur for an applied force equal to F^*.

Dynamic Measurements

Base Pair Dependence

We now present DFS measurements performed on complementary DNA strands of different length [10, 20, and 30 base pairs (bp)] and pulled apart at their opposite 5'-ends. The base sequences of the oligonucleotides were designed to favor the binding to complementary oligonucleotides in the ground state with respect to intermediate duplexes in which the strand is shifted relative to its complement. We have chosen the oligomer **a** (5'-G-G-C-T-C-C-C-T-T-C-T-A-C-C-A-C-T-G-A-C-A-T-C-G-C-A-A-C-G-G-3'),
which contains 30 bases and in which every three base motive occurs only once in the sequence. For this sequence, self-complementarity is avoided because the complement of each three-base motive is not contained in the sequence. **a** was tested against its complement **b** (30 bp) and against truncated components **c** (20 bp) and **d** (10 bp), respectively.

As expected, a F^* *versus* ln(v) plot shows a linear behavior for each duplex (Eq. 3, Fig. 2.). For each duplex, the distance Δx from the ground state to the energy barrier and the thermal off rate k_{off} were determined according to Eq. 3. The Δx distance was found to follow the linear relation:

$$\Delta x \approx \left[0.12 \;\; x \;\; n\right] \; nm,$$

where n is the number of base pairs. This increase of Δx with n clearly indicates cooperativity in the unbinding process. Measurements of k_{off} can be described by: $k_{off} \approx 10^{\alpha - \beta n}\, s^{-1}$, where $\alpha = 3 \pm 1$ and $\beta = 0.5 \pm 0.1$. The obtained k_{off} values are in good agreement with thermodynamical data [21]. Let us finally point out that an exponentional decrease of the thermal off-rate with the number of base pairs is expected because of the increase of the activation energy for dissociation (Eq. 1). However, the pre-factor τ_0 in Eq. 1 also strongly decreases with the number of base pairs because of the increasing number of degrees of freedom of the system.

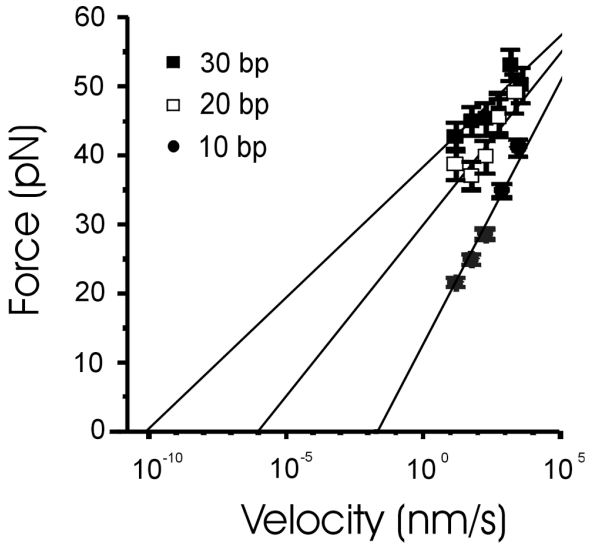

Fig. 2. *Velocity dependence of the most probable unbinding force [11]. Back squares (a-tip/b-surface, 30 bp), empty squares (a-tip/c-surface, 20 bp), circles (a-tip/d-surface, 10 bp). From a linear fit, both the force-scales $F^0 = k_BT/\Delta x$ and thermal off-rates can be determined.*

Temperature Dependence

In this section, preliminary temperature dependent DFS measurements are briefly discussed. The sequence **e** (5'-T-A-T-T-A-A-T-A-T-C-A-A-G-T-T-G-3') [22] attached to the tip and its complement **f** was immobilized on the surface. As previously, PEG linkers were used and DNA strands were pulled apart at their opposite 5'-ends. The specifity of the interaction was comparable to the one obtained in base-pair dependent measurements (Fig. 1.).
As seen in Fig. 3., the slope of the F^* versus ln(r) plots changes as a function of temperature, which provides

evidence for a strong temperature dependence of Δx. This result emphasizes the fact that for the DNA-duplex, the energy landscape is much more complicated than that of ligand-receptor bonds. As a consequence, the unbinding process may involve many different reaction paths. In this case thermal fluctuations are expected to play a key role.

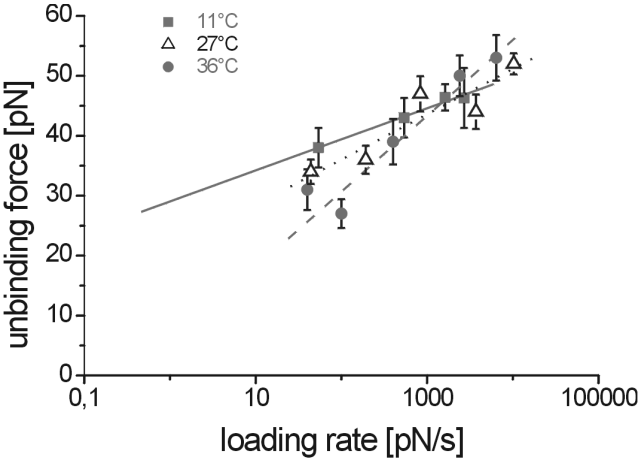

Fig. 3. *The most probable unbinding force as a function the loading rate (e-tip/f-surface, 16 bp) obtained at different temperatures. Squares (11 °C), triangles (27 °C), circles (36 °C).*

Conclusion

Using DFS measurements, the energy landscape of molecular bonds can be mapped. Moreover, relevant parameters such as the location and height of the barriers and the thermal off-rates can be determined. Our measurements confirm that the most probable force for unbinding scales as the logarithm of the loading rate. The base pair dependent measurements indicate that unbinding of DNA strands is a cooperative process. Temperature dependent measurements provide evidence for a decrease of Δx as the temperature increases. Since the limited range of loading rates available in an AFM experiment does not allow one to map the whole energy landscape, such experiments should be combined in the future with other DFS setups such as bio-membrane force probe or optical tweezers setups.

Acknowledgment: This work was supported by the Swiss National Science Foundation and the Treubel Foundation.

References

[1] Lee, G. U., Chrisley, L. A., Colton, R. J. Science **266** (1994) 771-773.
[2] Lee, G. U., Kidwell, D. A. Colton, R. J. Langmuir **10** (1994) 354-357.
[3] Moy, V. T., Florin, E. L., Gaub, H. E. Science **266** (1994) 257-259.
[4] Dammer, U., Popescu, O., Wagner, P., Anselmetti, D., Güntherodt, H. J., Misevic, G. N. Science **267** (1995) 1173-1175.
[5] Hinterdorfer, P., Baumgartner, W., Gruber, H. J., Schilcher, K., Schindler, H. Proc. Natl. Acad. Sci USA **93** (1996) 3477-3481.
[6] Dammer, U., Hegner, M., Anselmetti, D., Wagner, P., Dreier, M., Huber, W. and Güntherodt, H. J. Biophys. J. **70** (1996) 2437-2441.
[7] Allen, S, Chen, X. Y., Davies, J., Davies, M. C., Dawkes, A. C., Edwards, J. C., Roberts, C. J., Sefton, J., Tendler, S .J. B., Williams, P. M. Biochemistry **36** (1997) 7457-7463.
[8] Rief, M., Gautel, M., Oesterhelt, F., Fernandez, J. M., Gaub, H .E. Science **276** (1997) 1109-1112.
[9] Ros, R., Schwesinger, F., Anselmetti, D., Kubon, M., Schafer, R., Pluckthun, A., Tiefenauer, L. Proc. Natl. Acad. Sci USA **95** (1998) 7402-7405.
[10] Merkel, R., Nassoy, P., Lueng, A., Ritchie, K., Evans, E. Nature **397** (1999) 50-53.
[11] Strunz, T., Oroszlan, K., Schäfer, R., Güntherodt, H. J. Proc. Natl. Acad. Sci USA **96** (1999) 11277-11282.
[12] Schwesinger, F., Ros, R., Strunz, T., Anselmetti, D., Güntherodt, H. J., Honegger, A., Jermutus, L., Tiefenauer, L., Pluckthun, A. Proc. Natl. Acad. Sci USA **97** (2000) 9972-9977.
[13] De Paris, R., Strunz, T., Oroszlan, K., Güntherodt, H. J., Hegner, M. Single Mol. **1** (2000) 285-290.
[14] Evans, E., Leung A., Hammer D., Simon S. Proc. Natl. Acad. Sci USA **98** (2001) 3784-3789.
[15] Kramers, H.A. Physica Utrecht **7** (1940) 284-304.
[16] Bell, I., Science **200** (1978) 618-627.
[17] Evans, E. Annu. Rev. Biophys. Biomol. Struct. **30** (2001) 105-128.
[18] Galligan, E., Roberts C. J., Davies, M.C., Tendler S. J. B., Williams P.M., J. Chem. Phys. (2001) 3208-3214.
[19] Heymann, B., Grubmüller, H. Phys. Rev. Lett. **84** (2000) 6126-6129.
[20] Hutter, J.L., Bechhoefer, J. Rev. Sci. Instrum. **64** (1993) 1868-1873.
[21] Pörschke, D., Eigen, M. J. Mol. Biol. **62** (1971) 361-381.
[22] Tibanyenda, N., Debruin, S. H., Haasnoot, C. A. G., Vandermarel, G. A., Vanboom, J. H. Hilbers, C. W. Europ. J. Biochem. **139** (1984) 19-27.